Am J Cancer Res 2024;14(7):3584-3599
www.ajcr.us /ISSN:2156-6976/ajcr0158187

Original Article

Exploring doxorubicin transport in 2D and 3D models of MDA-MB-231 sublines: impact of hypoxia and cellular heterogeneity on doxorubicin accumulation in cells

Indrė Januškevičienė, Vilma Petrikaitė

Laboratory of Drug Targets Histopathology, Institute of Cardiology, Lithuanian University of Health Sciences, Sukilėlių av., LT-50162 Kaunas, Lithuania

Received May 31, 2024; Accepted July 12, 2024; Epub July 15, 2024; Published July 30, 2024

Abstract: Triple-negative breast cancer (TNBC) treatment is challenging due to its aggressive nature and heterogeneity of this type of cancer, characterized by various subtypes and intratumoral diversity. Doxorubicin (DOX) plays a crucial role in TNBC chemotherapy reducing the tumor size and improving patient survival. However, decreased drug uptake and increased resistance in specific cell subpopulations reduce the effectiveness of the treatment. This study explored the differences in DOX transport in MDA-MB-231 phenotypic sublines in cell monolayer (2D model) and cell spheroids (3D cultures). Cell spheroids were formed using magnetic 3D Bioprinting method. DOX transport into cells and spheroids was evaluated using fluorescence microscopy after different incubation durations with DOX in normoxia and hypoxia. In hypoxia, DOX transport into cells was 2.5 to 5-fold lower than in normoxia. The subline F5 monolayer-cultured cells exhibited the highest DOX uptake, while subline H2 cells showed the lowest uptake in normoxia and hypoxia. In 3D cultures, DOX transport was up to 2-fold lower in spheroids formed from subline H2 cells. Spheroids from subline D8 and MDA-MB-231 parent cells had the highest DOX uptake. A correlation was observed between the characteristics of the cells and their resistance to anticancer drugs. The results indicate that different cancer cell subpopulations in tumours due to differences in drug uptake could significantly impact treatment efficacy.

Keywords: Heterogeneity, cell sublines, drug resistance, doxorubicin transport, tumor spheroids, hypoxia

Introduction

Treatment of triple-negative breast cancer (TNBC) is a huge challenge in oncology. This cancer type is characterized by the absence of estrogen receptors (ER), progesterone receptors (PR) and human epidermal growth factor receptors-2 (HER2), which precludes the possibility of using hormone therapies and HER2-targeted treatments, leaving chemotherapy as the primary treatment option. Due to its effectiveness in killing cancer cells, doxorubicin (DOX) is frequently employed among chemotherapeutic agents. However, the heterogeneity inherent in TNBC, both at the intertumoral and intratumoral levels, significantly complicates the therapeutic strategy, decreasing the efficacy of anticancer agents such as DOX [1]. The complexity of TNBC is further amplified by the tumour microenvironment (TME), a dynamic ecosystem comprising not only the cancer cells but also various non-cancerous cell types, including fibroblasts, immune cells, and endothelial cells. It is known that interaction between cancer cells and TME might affect tumour progression. However, little information exists about phenotypically different cancer cell interactions in tumours. Cell-cell interactions are mediated by a complex network of signaling pathways and physical contact, making cell interaction a critical factor in developing effective treatment strategies for TNBC [2].

Scientists have extensively studied the transport of DOX in both cell monolayers and spheroids (3D cultures). The key factors known to impede DOX transport in cancer cells include overexpression of efflux pumps [3], intracellular sequestration of drugs in subcellular compartments such as lysosomes [4], pH changes with-

https://doi.org/10.62347/VNWH9165

in cancer cells [5], interactions of cancer cells with TME [6-8] and, notably, interactions among phenotypically distinct cancer cells within the tumour [9, 10]. It is recognized that interactions between different cancer cell phenotypes can contribute to cancer progression and drug resistance [11-14]. To our knowledge, no studies have specifically addressed the interactions between phenotypically diverse cancer cells in relation to drug resistance. Although many publications have reported on the isolation and characterization of different sublines, populations, or clones [15-18], their interactions have not been explored regarding DOX transport.

Given the critical role of the cell-cell interaction in cancer progression and treatment response, this study focuses on the DOX transport into the MDA-MB-231 cell line and its phenotypically diverse sublines (D8, F5, H2). The DOX transport was investigated in cell monolayer (2D model) and spheroids (3D cultures). To mimic cell interaction *in vivo* conditions, apart from 3D cultures, experiments in monolayer-cultured cells were done under normoxia and hypoxia. Hypoxia, a common feature of the tumour, is known to influence the biology of cancerous and stromal cells, affecting drug uptake and, consequently, treatment efficacy [19, 20].

This research hypothesized that by studying DOX transport in conditions that simulate the complex environment of tumors in living organisms, we could identify obstacles to effective drug delivery and uncover strategies to enhance treatment results for patients with TNBC. The significance of this work lies in its potential to contribute to the refinement of therapeutic regimens for TNBC, a subtype of breast cancer known for its poor prognosis and limited treatment options. This could pave the way for developing more effective, personalized treatment strategies considering the complex interplay between cancer cells and their microenvironment.

Materials and methods

Cell culture

The human triple-negative breast cancer cell line MDA-MB-231 was acquired from the American Type Culture Collection (ATCC) located in Manassas, VA, USA. Similarly, human foreskin fibroblast cells (HF) CRL-4001, originally sourced from ATCC, were generously provided by Prof. Helder Santos from the University of Helsinki, Finland. These cell lines were cultured in Dulbecco's Modified Eagle Medium (DMEM) GlutaMAX supplied by Gibco, UK, and enriched with 10% fetal bovine serum (FBS), heat-inactivated (Gibco). Additionally, the culture medium was supplemented with 1% of penicillin and streptomycin mixture, 1 µg/ml of insulin (27 USP units/mg), 1% minimum essential medium non-essential amino acids (MEM NEAA), and 1% sodium pyruvate, all supplied from Gibco, UK. Cells were cultured in a humidified environment with 5% CO_2 at a temperature of 37°C.

Isolation of cell sublines from commercial MDA-MB-231 cell line

Sublines were derived from the MDA-MB-231 commercial cell line, utilizing a previously described method involving serial dilution in 96-well plates [21]. Initially, an 8-channel micropipette was used to dispense 100 µl of the medium into each well of a 96-well plate, excluding well A1. Subsequently, 200 µl of a cell suspension (containing 2×10^4 cells/ml) was introduced into well A1. From there, 100 µl of this mixture was transferred from well A1 to B1 using a single channel pipettor, a process repeated down the column, with the final 100 µl from well H1 being discarded. Next, each well in column 1 received an additional 100 µl of medium via the 8-channel micropipette, bringing the total volume to 200 µl per well. This dilution was then extended horizontally across the plate, transferring 100 µl from each well in the first column to the corresponding wells in the second column using the same micropipette, and the process was replicated across the plate. Following nine days of incubation, cell colonies were observed under a microscope. The selection of sublines was based on the observed differences in colony formation, including shape and cell density. Selected wells were then expanded into 25 cm^2 cell culture flasks (TPP, Switzerland) for further cultivation.

DOX cytotoxicity by MTT

Cell susceptibility to DOX was determined using the MTT assay, as described previously [22]. Fresh DOX dilutions in the medium were prepared just before use. DOX (> 98%, Abcam, Cambridge, UK) was dissolved in dimethyl sulf-

oxide (DMSO, Sigma-Aldrich Co., St. Louis, MO, USA) and then diluted in the medium, ensuring the final DMSO concentration did not exceed 0.5%. Cells (2×10^4 cells/well) were plated into 96-well flat-bottomed plates and incubated for 24 h. Subsequently, DOX dilutions were added to each well. The medium without cells served as a positive control, and the medium with 0.5% DMSO served as a negative control. After 4 and 8 hours of incubation, 20 µl of 3-(4,5-dimethylthiazol2-yl)-2,5-diphenyltetrazolium bromide (MTT, Life technologies, Oregon, USA) solution (5 mg/ml in medium) was added. Following a 3-hour incubation at 37°C, the liquid was removed, and the resulting formazan crystals were dissolved in 50 µl of DMSO. Complete solubilization of formazan crystals was achieved by brief shaking. The absorbance was measured on a plate reader at 570 and 630 nm.

DOX transport into monolayer-cultured cells

The cells were seeded in 24-well plates on collagen-coated coverslips at a volume of 500 µL (50,000 cells/well) and incubated for 48 h in a humidified atmosphere with 5% CO_2 at 37°C. After 48 h, the medium was replaced by the fresh medium that contained 1 or 5 µM DOX. In case to simulate hypoxia, the medium containing 200 µM cobalt (II) chloride (anhydrous, 97%, Carl Roth GmbH, Germany), was used. After 0.5, 1, 2 or 4 h of incubation, the medium was removed, the cells were washed twice with PBS, fixed with 4% paraformaldehyde (Thermo Scientific, Waltham, MA, USA) solution in PBS and stained with 4',6-diamidino-2-phenylindole (DAPI; Thermo Scientific). The photos were taken using confocal fluorescence microscopy (Olympus IX73, Japan), 600 × magnification, using DAPI and TRITC filters. The uptake of DOX into whole cells and their nucleus was evaluated using *ImageJ* software (National Institutes of Health, 1.53K version, USA). In each group, at least 5 photos were taken, and from these photos, 20 randomly selected cells were analyzed. The relative fluorescence intensity and background fluorescence were measured separately for the cytoplasm and nuclei, and the background fluorescence was subtracted from the cellular fluorescence measurements. The same procedure was followed for experiments conducted under hypoxic conditions. To induce hypoxia, 200 µM cobalt (II) chloride was added to the culture medium 24 hours prior to the experiment.

DOX delivery into tumor spheroids

The spheroids were formed using the magnetic 3D Bioprinting method as previously described [21]. Cells were seeded in a 6-well plate, and after their attachment, they were incubated with NanoShuttle PL (Greiner Bio-One North America, Inc., Monroe, NC, USA) for 8-10 h. Then, cells were trypsinised, centrifuged, resuspended in a fresh medium and seeded into 96-well ultra-low attachment plates in a volume of 100 µL (2000 cancer cells (MDA-MB-231 or sublines D8, F5, H2) and 2000 human fibroblasts). The plate was placed on a magnetic drive and incubated in a humidified atmosphere containing 5% CO_2 at 37°C for 2 days. After that, the medium was replaced with a fresh medium containing 10 µM of DOX. After 1, 2, 4 and 8 h, spheroids were washed with PBS and fixed in a 4% paraformaldehyde solution in PBS. DOX transport to the spheroids was assessed by fluorescence microscopy with an Olympus IX73 inverted fluorescent microscope (Olympus, Tokyo, Japan). The images were analyzed using *ImageJ* software version *1.53K* to estimate the intensity of DOX fluorescence in the whole spheroids area in relative units. The DOX fluorescence intensity in the spheroids is calculated by subtracting the background fluorescence measured at multiple places near the spheroid. The number of spheroids per group ranged from 10 to 14 spheroids.

Statistical analysis

Each experiment was conducted in triplicate, with the results averaged and the standard deviation calculated. Data analysis was done utilizing Microsoft Office Excel 2021, 2405 version (Microsoft Corporation, Redmond, WA, USA) and the IBM SPSS Statistics software, version 26.0. A value of $P < 0.05$ was considered as the level of significance. An analysis of variance (ANOVA) was applied to identify significant differences among the values, followed by a Tukey post-hoc test for detailed comparison.

Results

Selection of sublines isolated from the MDA-MB-231 cell line for DOX uptake studies

In previous studies focused on the interactions of phenotypically different sublines [21], we isolated 24 sublines and selected seven (A9, D8,

E7, F5, F7, G5, and H2) for characterization based on CD133 receptor expression, migratory ability, and sensitivity to the anticancer drugs doxorubicin (DOX) and paclitaxel (PTX). Among these, we identified three sublines - D8, F5, and H2 - as the most distinct. The D8 subline exhibited a 50% reduction in CD133 expression, a 20% increase in migratory ability, and a 10% greater sensitivity to PTX. Morphologically, D8 cells were elongated and loosely packed. The F5 subline showed a 31% increase in CD133 expression, a 5% decrease in migratory ability, and a 54% higher sensitivity to DOX. These cells were shorter, more oval, and formed tightly packed colonies. The H2 subline was notable for its resistance to anticancer drugs, with 39% lower sensitivity to DOX and 32% lower sensitivity to PTX. Additionally, H2 cells exhibited a 38% increase in migratory ability and a 26% reduction in CD133 expression compared to the parental MDA-MB-231 cell line. The H2 cells were also shorter in shape compared to the parental cells.

DOX uptake in phenotypically different breast cancer sublines in normoxia

In this research, it was hypothesized that varying concentrations of DOX (1 μM and 5 μM) will elicit different patterns of intracellular uptake in cells. Specifically, in this study, it was supposed that at the lower concentration (1 μM), DOX uptake would be relatively evenly distributed between the cytoplasm and nucleus. Conversely, at the higher concentration (5 μM), it will anticipate increased transport and accumulation of DOX within the nucleus, which is a main DOX target in cancerous cells.

Before conducting DOX transport experiments, it is important to assess the influence of DOX on cell viability to ensure that changes in DOX uptake are not solely due to the drug's cytotoxic effects. In this experiment, a statistically significant DOX cytotoxicity effect on cell viability was not established up to a concentration of 10 μM after 8 hours of incubation (**Figure 1**).

DOX transport in MDA-MB-231 cells and its sublines D8, F5, H2 was first explored in normoxia conditions (**Figure 2C**). At 1 μM concentration, DOX uptake was highest in subline F5 cells after 240 minutes (**Figure 2A**). DOX delivery in F5 cells and nucleus was up to 1.8-fold and 1.5-fold greater, respectively, compared to other sublines and parent MDA-MB-231 cell line (**Figure 2B**). Contrary, the H2 subline showed the least 1.5-fold lower DOX uptake among all the cell lines and sublines tested, highlighting significant variability in drug uptake efficiency among different cellular phenotypes.

The DOX uptake ratio between cells and nucleus was the same in MDA-MB-231 and sublines (**Figure 3C**). Cells incubated with 5 μM DOX show increased DOX uptake and accumulation in the cell nucleus (**Figure 3B**). The subline F5 cells continued to exhibit a superior capacity for DOX uptake, with uptake levels in both the cells and their nuclei about 1.5-fold higher than those observed in other cell lines and sublines (**Figure 3A**, **3B**). The DOX transport into subline H2 cells was about 2-fold lower in both cells and nuclei than the subline F5 and about 1.5-fold lower than the parent cell line MDA-MB-231.

In this research, no statistically significant DOX uptake was observed in the cells or their nuclei after 30, 60, and 120 minutes of incubation across all compared cell lines and sublines.

However, differences in DOX distribution within the cells were observed when comparing DOX uptake in cells using 1 μM or 5 μM concentrations. At 1 μM of DOX, similar drug distribution was observed between the cell cytoplasm and nucleus, with DOX uptake in the nucleus being 1.7-fold higher than in the cytoplasm. Conversely, at a concentration of 5 μM, DOX distribution within the cell and nucleus differed significantly, with DOX uptake in the cell nucleus being 2.6-fold higher than in the cytoplasm. The highest difference was observed in the H2 subline, where DOX uptake in the cell nucleus was 3.2-fold higher than in the cytoplasm.

DOX uptake in phenotypically different breast cancer sublines in hypoxia

Analyzing DOX transport under hypoxic conditions is crucial for understanding how an oxygen-deprived environment affects DOX uptake efficiency. In this study, differences in DOX uptake and uptake ratios were observed between hypoxic and normoxic conditions. Moreover, the effects of different DOX concentrations varied between normoxia and hypoxia. DOX uptake under hypoxic conditions was approximately 5-fold lower at 1 μM and 2-fold lower at 5 μM compared to normoxic conditions (see **Figures 4** and **5**).

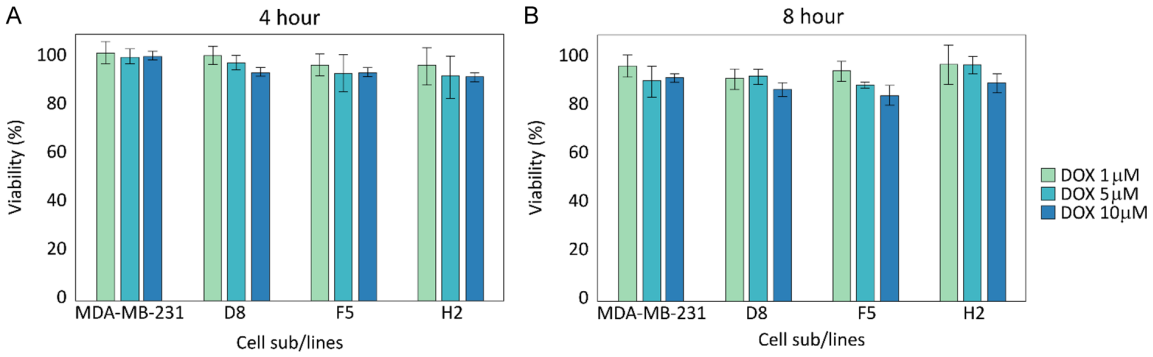

Figure 1. DOX effect on cell viability. Viability was evaluated in monolayer-cultured cells of MDA-MB-231 cell line and its sublines after incubation with 1, 5 or 10 μM DOX. A. Viability of cells after 4 hours of incubation. B. Viability of cells after 8 hours of incubation, n = 3.

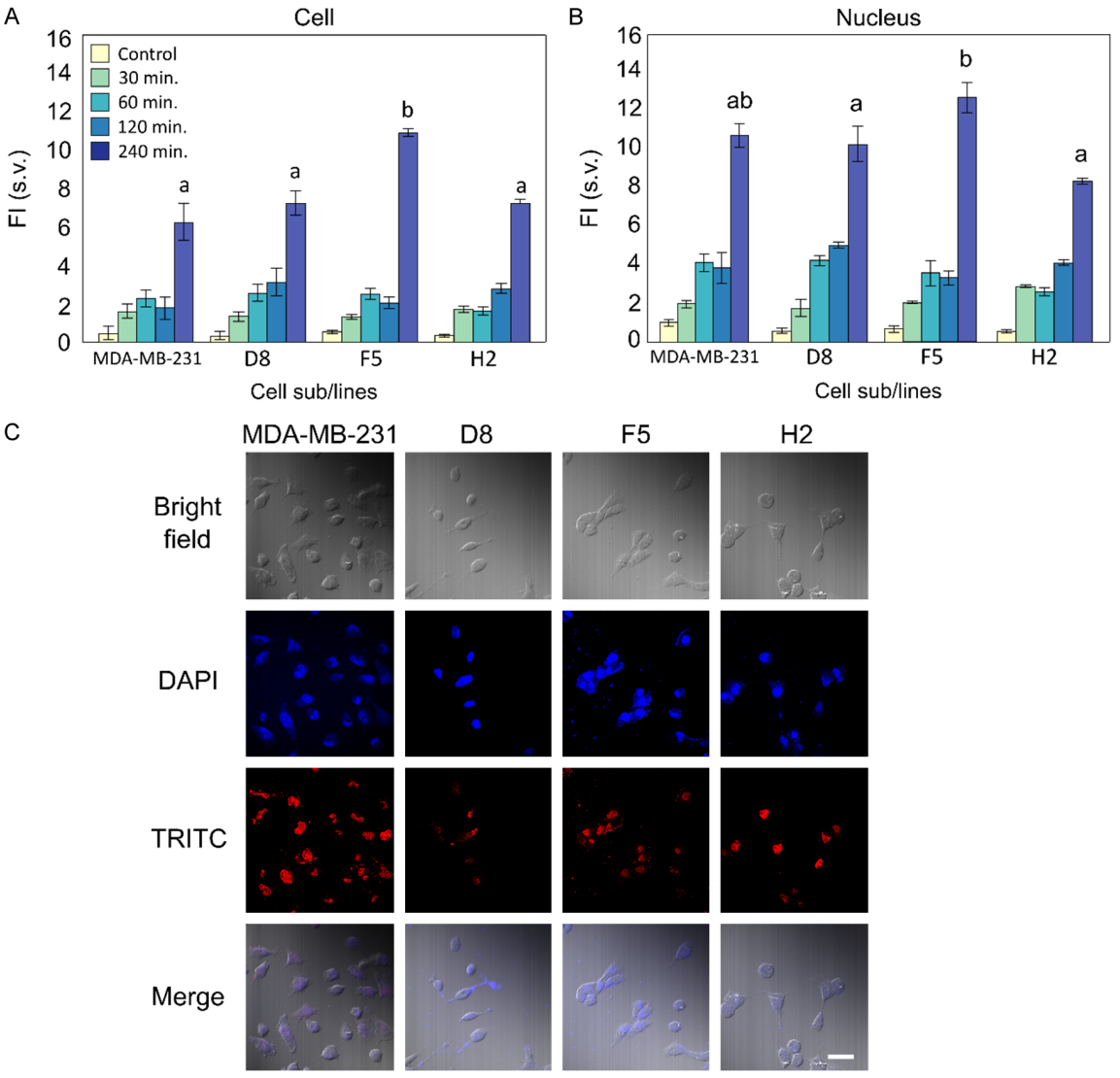

Figure 2. DOX uptake into monolayer-cultured cells from MDA-MB-231 cell line and its sublines after incubation with 1 μM DOX in normoxic conditions. A. DOX fluorescence intensity in cells. B. DOX fluorescence intensity in cell nucleus at different time periods. C. Representative images of cells after 4 h incubation with 1 μM DOX. Scale bar = 50 μm. Bars marked with different letters indicate statistically significant differences ($P < 0.05$) within the same category, n = 3.

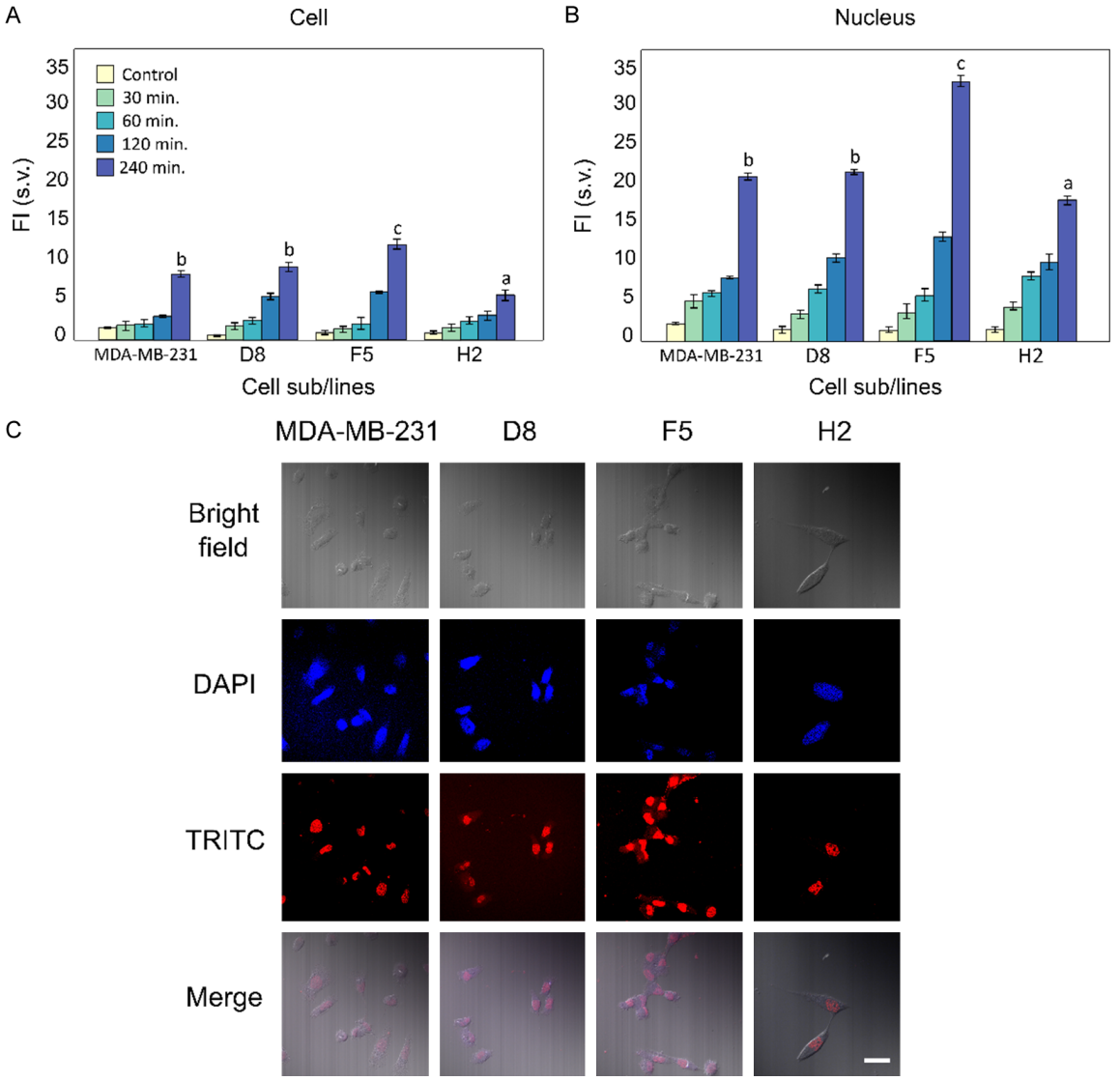

Figure 3. DOX uptake into monolayer-cultured cells from MDA-MB-231 cell line and its sublines after incubation with 5 μM DOX in normoxic conditions. A. DOX fluorescence intensity in cells. B. DOX fluorescence intensity in cell nucleus at different time periods. C. Representative images of cells after 4 h incubation with 5 μM DOX. Scale bar = 50 μm. Bars marked with different letters indicate statistically significant differences ($P < 0.05$) within the same category, n = 3.

The F5 subline demonstrated the highest DOX fluorescence intensity among the cell lines tested after 240 minutes of incubation with 1 μM DOX (**Figure 4A**). This intensity was approximately 2.5-fold higher than observed in the H2 subline and 2-fold higher than in the MDA-MB-231 and D8 sublines, as illustrated in **Figure 4C**. Comparatively, under these oxygen-deprived conditions, no significant differences were noted in the uptake of DOX into the nuclei of the cells across the different sublines (**Figure 4B**).

When the DOX concentration was increased to 5 μM, an enhanced DOX uptake into cells and nuclei was observed, as represented in **Figure 5C**. After 240 minutes of incubation, the DOX fluorescence intensity in cells of the MDA-MB-231, F5, and D8 sublines showed no statistically significant differences at this higher concentration. However, the DOX fluorescence intensity in H2 subline cells remained approximately 1.7-fold lower than in the other examined subline cells (**Figure 5A**). Furthermore, the overall DOX fluorescence intensity under hypox-

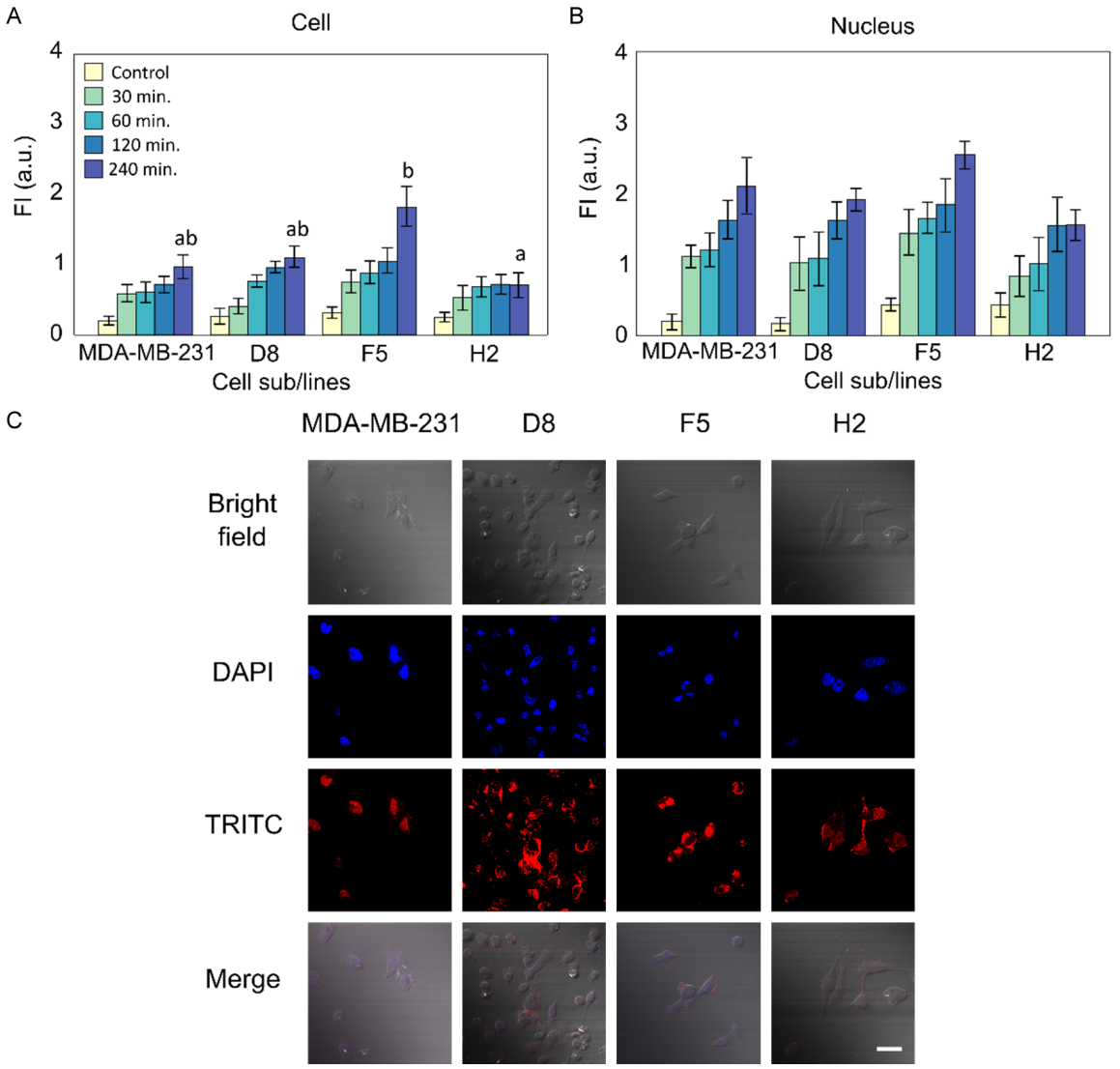

Figure 4. DOX uptake into monolayer-cultured cells from MDA-MB-231 cell line and its sublines after incubation with 1 μM DOX in hypoxic conditions. A. DOX fluorescence intensity in cells. B. DOX fluorescence intensity in cell nucleus at different time periods. C. Representative images of cells after 4 h incubation with 1 μM DOX. Scale bar = 50 μm. Bars marked with different letters indicate statistically significant differences ($P < 0.05$) within the same category, n = 3.

ic conditions was 2.5-fold lower than that under normoxic conditions for the same DOX concentration. The study also highlighted a more pronounced DOX transport into the nuclei, approximately 2-fold higher than in the cytoplasm of the cells (**Figure 5B**), with the highest DOX transport observed in the nuclei of F5 subline cells. Notably, DOX transport into cell nuclei was 3-fold lower under hypoxic compared to normoxic conditions.

However, when comparing DOX uptake in cells at 1 μM or 5 μM concentrations in hypoxic environment, differences in DOX distribution within the cells were observed. At 1 μM of DOX, a different drug distribution between the cell cytoplasm and nucleus was observed, with DOX uptake in the nucleus being from 1.4 to 2.2-fold higher than in the cytoplasm. The same tendency was observed at a concentration of 5 μM. The DOX distribution within the cell and nucleus, with DOX uptake in the cell nucleus being from 2 to 3.9-fold higher than in the cytoplasm. The highest difference was observed in the H2 subline, where DOX uptake in the cell nucleus was 3.8-fold higher than in the cell cytoplasm.

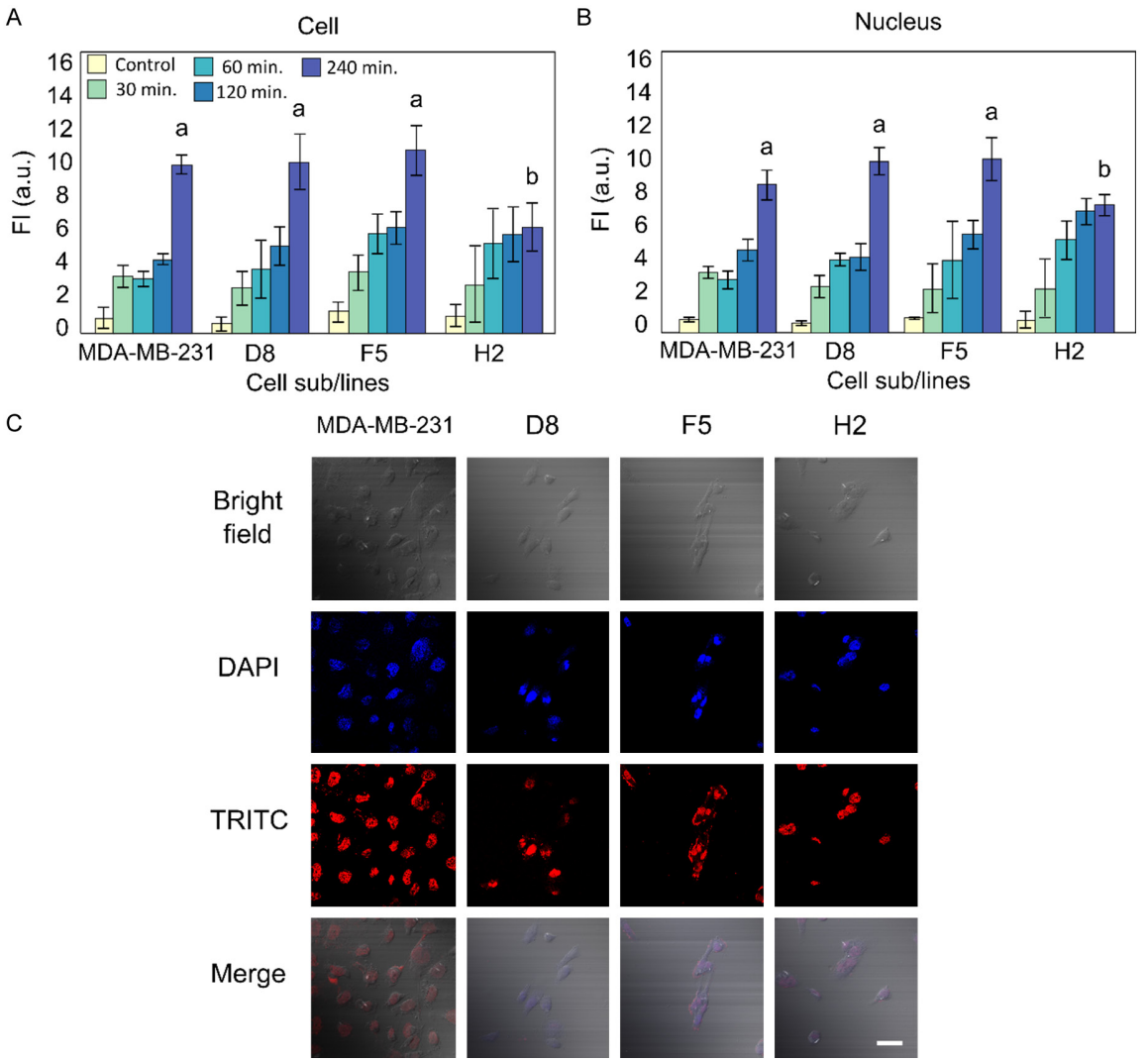

Figure 5. DOX uptake into monolayer-cultured cells from MDA-MB-231 cell line and its sublines after incubation with 5 μM DOX in hypoxic conditions. A. DOX fluorescence intensity in cells. B. DOX fluorescence intensity in cell nucleus at different time periods. C. Representative images of cells after 4 h incubation with 5 μM DOX. Scale bar = 50 μm. Bars marked with different letters indicate statistically significant differences ($P < 0.05$) within the same category, n = 3.

DOX transport into spheroids

MDA-MB-231 cells alone did not form spheroids, so HF (fibroblast) cells were used. Combining breast cancer cells with fibroblasts when forming spheroids allowed us to better mimic the TME.

The spheroids formed at the experiment's onset had an average diameter of approximately 390 μm. Across the groups, spheroid sizes varied between 360 and 420 μm. The largest spheroids, lacking a clear round shape, were formed by D8 subline cells, while the smallest were observed in the H2 subline cells. Spheroid sizes remained consistent within each group under control and DOX incubation conditions.

Fluorescence intensity demonstrated that the penetration of DOX into the cell spheroids was directly proportional to the duration of incubation, highlighting a time-dependent penetration mechanism (**Figure 6B**). After 1 hour of incubation, DOX transport into MDA-MB-231 spheroids was up to 1.5-fold higher than in other groups, though not statistically significant (**Figure 6A**). After 8 hours of incubation, the penetration of DOX was higher in spheroids

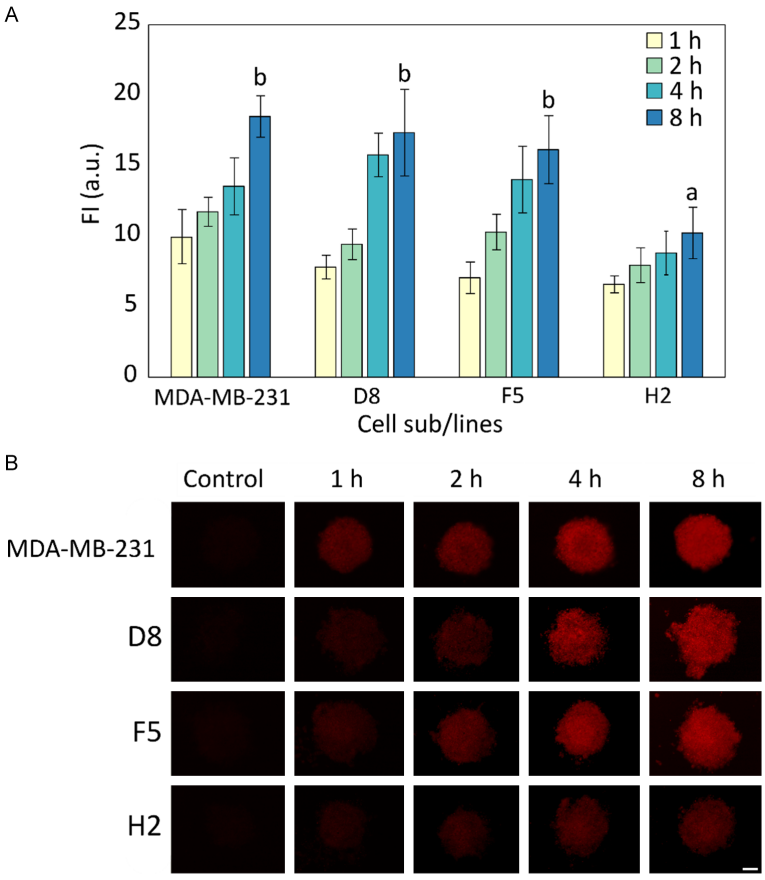

Figure 6. The different DOX penetration into spheroids at DOX 10 μM concentration. DOX fluorescence intensity in spheroids at different time periods (A), images of cells after 8 h incubation with DOX (B). Magnification 100 ×. Scale bar = 100 μm. *The different letters indicate P < 0.05 compared the DOX penetration at the same time in different cell sublines*, n = 3. Abbreviation: MDA, MDA-MB-231 cell line.

formed from subline D8, F5, and MDA-MB-231 cells than from subline H2 cells. DOX fluorescence intensity in spheroids from subline H2 cells was about 2-fold lower than in the other spheroids (**Figure 6A**). These findings are consistent with the results from studies in 2D cultures.

Discussion

Triple-negative breast cancer is recognized for its inherent heterogeneity, a characteristic that complicates treatment strategies. This diversity within TNBC tumours contributes to the emergence of drug resistance, driven by the phenotypic variations among subpopulations. Current scientific research delves deeply into understanding these differences among sublines and their interactions to decipher their influence on treatment outcomes [1].

This study investigates the heterogeneous nature of TNBC, focusing on the variations in DOX uptake among different sublines, which are associated with distinct traits such as drug resistance (H2 subline), CD133 receptor expression (F5 subline), and migration rates (D8 subline), consistent with previous findings [21]. Furthermore, we examine the influence of culture conditions, particularly the contrast between normoxic and hypoxic environments, on DOX uptake, aiming to elucidate the underlying mechanisms contributing to DOX resistance in TNBC. Studies have demonstrated significant differences in DOX uptake among these sublines. For example, Bao et al. [23] demonstrated substantial differences in DOX, with DOX primarily accumulating in the nucleus of the DOX-sensitive MDA-MB-231 subline, while in the resistant subline, it predominantly resided in the cytoplasm. Further, recent research by Khan et al. [24] indicated that single cell-derived clones from four different breast cancer cell lines exhibited varied sensitivities to DOX. These findings highlight the necessity of assessing DOX uptake in phenotypically different sublines, as this can provide pivotal insights into overcoming DOX resistance in cancer treatment.

During the investigation of DOX penetration into cells cultured in monolayers, significant variations in DOX penetration were evident. Primarily, distinct differences in DOX penetration were noted among MDA-MB-231 sublines. Additionally, the variations of DOX distribution in the cell cytoplasm and nucleus were determined. Subsequently, environmental conditions, such as normoxia and hypoxia, were observed to impact the intracellular entry of

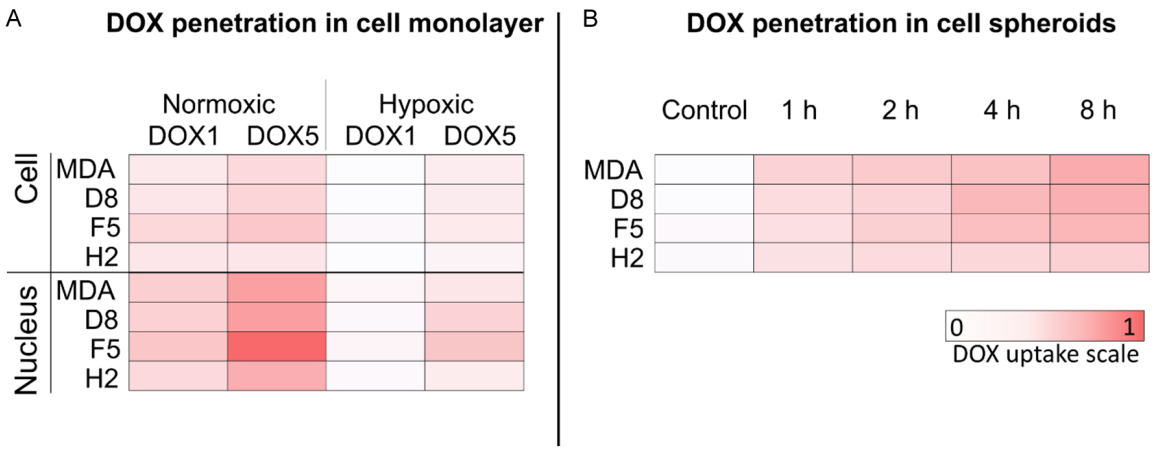

Figure 7. Comparing DOX uptake in 2D and 3D cell cultures. A. DOX uptake in monolayer cultured cells after 8 hours of incubation. B. DOX transport into spheroids at incubation periods from 1 to 8 hours. The scale bar represents normalized DOX fluorescence intensity (FI). The highest amount of FI equal to 1.

DOX, which was an expected result. The observed decrease in DOX uptake under hypoxic conditions significantly impacts chemotherapy's effectiveness, particularly in the microenvironments of rapidly growing tumours with low oxygen supply. Hypoxia-inducible factors (HIFs), especially HIF-1, play a crucial role in this process, activating drug resistance mechanisms like P-glycoprotein and altering gene transcription to promote tumour survival and growth, thereby reducing the intracellular concentration of anticancer drugs such as DOX [20, 25]. Our findings reveal that in hypoxic conditions, DOX uptake in both cells and their nuclei substantially decreases up to five times with a lower concentration and almost three times with a higher concentration, compared to normoxic conditions. This reduction in DOX uptake underlines the adaptability of breast cancer cells, such as the MDA-MB-231 line, to hypoxic conditions by modifying their metabolism to not only survive but also expel chemotherapeutic drugs.

In the present study, subline F5 cells demonstrated the most pronounced uptake of DOX under normoxic conditions (**Figure 7A**), with an increased uptake observed under hypoxic conditions with elevated DOX concentrations. Previously recognized as notably responsive to DOX [21], the F5 subline exhibited a higher accumulation of DOX within both cytoplasmic and nuclear compartments, correlating with increased cellular sensitivity to the drug. Additionally, scientists noted divergent resistance patterns to DOX across various sublines of the MDA-MB-231 cell line [24]. At the DOX uptake experiments, an increased fluorescence intensity was observed in the F5 subline nucleus. This observation indicates that in DOX-sensitive cells, DOX efficiently localizes in higher concentrations in the cell nucleus and less in the cytoplasm [23]. The increased accumulation of DOX in the cell nucleus is primarily due to its ability to intercalate into DNA, aided by its hydrophilic nature and possibly active transport mechanisms that facilitate its entry and retention in the nucleus [26-28]. Typically, there is low expression of nuclear and cytoplasmic P-gp in DOX-sensitive cells, which results in an increased intracellular concentration of DOX [29, 30]. Comparing the DOX uptake results in F5 subline cells under hypoxia and normoxia, a threefold decrease in nuclear DOX uptake at a higher DOX concentration under hypoxia compared to normoxia suggests that tumours with cell phenotypes like the F5 subline may display increased resistance to chemotherapy in hypoxic conditions. This resistance poses a significant challenge, especially in tumours larger than 100 μm from the nearest blood vessel, as they are difficult to detect early due to their small size [25].

The H2 subline cells displayed the lowest DOX uptake between all tested lines (**Figure 7A**) under normoxia and hypoxia in the cells and their nuclei across both concentrations. This reduced uptake is consistent with the H2 subline's previously observed resistance to DOX

[21]. In DOX-resistant cells, DOX is typically unable to reach the nucleus and remains exclusively in the components of cytoplasm (mitochondria [31], endoplasmic reticulum [32] and lysosomal accumulation [33]), especially at lower concentrations [23]. However, at higher concentrations, DOX can cross the nuclear membrane pores in cells (passive diffusion [34] or active transport [35]) and exhibit increased fluorescence intensity in the nucleus compared to the cytoplasm. Additionally, the H2 subline showed a marked decrease in DOX uptake under hypoxia, 7-fold less in cells and 5-fold less in the nucleus than under normoxic conditions, highlighting the significant challenge hypoxia poses to effective cancer treatment.

The MDA-MB-231 and D8 subline cells displayed intermediate levels of DOX uptake under various growth conditions and DOX concentrations, ranking between the F5 and H2 sublines regarding uptake intensity into cells and nuclei under normoxic conditions. This observation underscores the similarity of the D8 subline to the MDA-MB-231 parent cell line. Our previous research has shown that D8 subline cells are more sensitive to anticancer drugs than the MDA-MB-231 cells, but in DOX uptake, significant differences were not determined.

Furthermore, our investigation of DOX transport in 3D cell cultures provides deeper insights into the complexities of drug delivery within the TME. 3D tumour spheroids can replicate the *in vivo* resistance patterns seen in solid tumours, attributed to factors such as hypoxia, cellular heterogeneity, and the physical barriers to drug diffusion [36]. Employing fibroblasts allowed us to model the TME more accurately and assess DOX transport in spheroids [37]. The observed time-dependent DOX transport in 3D cultures varied among MDA-MB-231, F5, D8, and H2 sublines, with H2 spheroids exhibiting the lowest DOX uptake compared to MDA-MB-231, F5, and D8 spheroids (**Figure 7B**). This underscores the critical role of different subline phenotypes in drug transport and resistance mechanisms. The spheroids from subline F5 cells exhibited a sensitivity to DOX, challenging the conventional understanding that cancer stem cell-like phenotypes (as indicated by high CD133 expression) are inherently resistant to chemotherapy. This F5 cell sensitivity in 3D cultures may point to the heterogeneity within the MDA-MB-231 cell line itself and suggests that not all cells with stem-like features exhibit the same drug resistance profiles [38-40]. The lower DOX uptake in H2 spheroids highlights the challenge of overcoming drug resistance in tumour subpopulations that exhibit reduced drug accumulation, potentially due to enhanced efflux mechanisms or alterations in drug metabolism pathways [41]. Our findings align with recent studies indicating that the microenvironment of solid tumours plays a significant role in modulating drug uptake and efficacy [42]. The reduced uptake of DOX in hypoxia observed in our study corroborates the notion that hypoxia-induced factors contribute to cancer drug resistance [25].

The variation in DOX uptake under normoxic versus hypoxic conditions highlights the significant influence of the TME on chemotherapy efficacy. This finding is consistent with the research by Gilkes et al. [43], which showed how hypoxia-inducible factors (HIFs) modulate gene expression to enhance survival and resistance in low-oxygen environments. Our study builds on this by demonstrating how these specific microenvironmental conditions directly affect drug uptake in TNBC cells. Additionally, using 3D spheroid models has revealed the challenges posed by complex tumour structures in drug delivery. Notably, the differential DOX uptake observed in 3D spheroids, particularly the reduced uptake in H2 subline spheroids, underscores the significant physical and biological barriers that complicate effective treatment. These observations are supported by findings from Weigelt et al. [44], who discussed the advantages of 3D models in replicating tumours' spatial and architectural heterogeneity, greatly affecting treatment outcomes.

Our study demonstrates a correlation between our results on DOX transport in 2D and 3D cultures and our previous research on DOX activity for cell viability and spheroid size reduction (**Figure 8**) [21].

Previously, we revealed that H2 subline cells were resistant to DOX. In this study, H2 cells showed the lowest DOX uptake compared to all other tested cells in both 2D and 3D cultures. Additionally, the viability of H2 subline cells was the highest compared to all tested sublines,

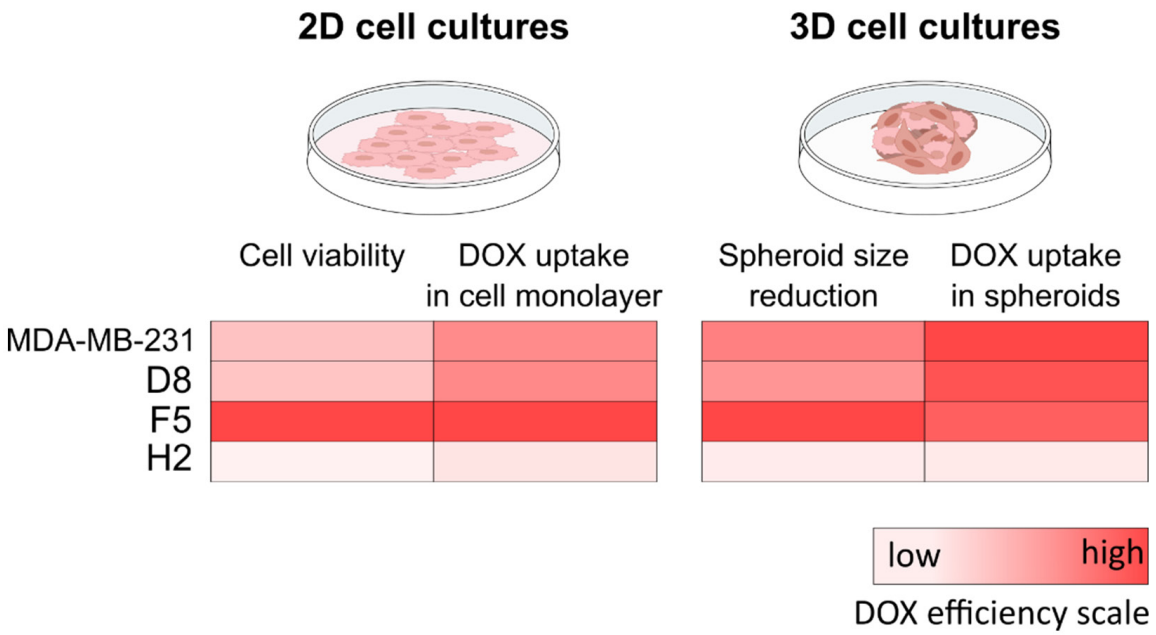

Figure 8. Comparison of DOX activity and transport in 2D and 3D cell cultures. In 2D cell cultures, the effect of DOX on cell viability was determined using the MTT-colorimetric method, while DOX uptake in cell monolayers was assessed through fluorescence intensity measurements. In 3D cell cultures, the reduction in spheroid size was measured (μm), and DOX uptake in spheroids was evaluated using fluorescence intensity. The scale bar represents relative units of the DOX effect in cells, ranging from low (light red) to high (intense red).

indicating the low effect of DOX (**Figure 8**, left). However, H2 subline spheroids showed the lowest DOX uptake, a finding that correlates with the results from 2D cell cultures. This may be attributed to insufficient drug accumulation in H2 cells, compromising its cytotoxic effects. Such a scenario could arise from several resistance mechanisms, including increased drug efflux, which actively removes the drug from the cell [23, 45, 46], and reduced drug influx. The resistance observed in the H2 subline could be associated with the TNBC mesenchymal subtype, known for its increased expression of multidrug resistance (MDR) pumps [47, 48]. This hypothesis is supported by the low DOX transport observed, suggesting that the H2 subline may have elevated MDR pump expression, a characteristic feature of the TNBC mesenchymal subtype.

The sensitivity of the F5 subline to DOX is due to high DOX accumulation in the nucleus of F5 cells (**Figure 7**, intense red colour). Furthermore, DOX statistically significantly reduced the size of the spheroids, and DOX entry into the spheroids of the F5 subline was the highest among all lines (**Figure 8**, right). Similar TNBC subtypes to the F5 subline may increase DOX transport in cells due to genetic or epigenetic modifications impairing efflux pumps' effectiveness, allowing DOX to remain within the cells longer [49, 50]. Additionally, this could lead to changes in lipid metabolism or membrane fluidity, affecting drug permeability. Finally, these cells might exhibit susceptibility to DOX's mechanism of action, such as intercalation into DNA and disruption of topoisomerase II, leading to effective cytotoxicity despite a stem-like phenotype [40]. These insights into the drug dynamics within the F5 subline could inform targeted strategies to overcome drug resistance in other TNBC subtypes exhibiting similar characteristics.

Many scientists are looking for effective inhibitors to reduce drug resistance in cancer cells [51-54] and evaluating different resistance mechanisms to DOX [55]. This research contributes to these findings and provides several insights that could significantly influence future treatment strategies. Identifying sublines with varying DOX uptake enables the development of targeted treatments, as sublines like F5, which uptake more DOX, respond better to DOX-based therapies, while resistant sublines, like H2, may require alternative or combination

treatments. Understanding the mechanism behind reduced DOX uptake in resistant sublines is essential for overcoming drug resistance therapies for specific tumor subpopulations and can enhance chemotherapy effectiveness. Understanding the mechanisms behind reduced DOX uptake (overcoming drug resistance) in resistant sublines is crucial. Factors like hypoxia reduce DOX uptake, implicating HIFs and efflux pumps like P-gp. Combining DOX with HIF inhibitors or P-glycoprotein blockers may enhance drug sensitivity in resistant sublines. The tumor microenvironment influence, such as normoxia and hypoxia, significantly affects DOX uptake. Hypoxic conditions notably reduce DOX penetration. Designing treatments that consider microenvironmental factors or target hypoxic tumor regions could enhance treatment efficacy. Also, phenotypic markers correlating with DOX uptake can serve as predictive biomarkers, helping stratify patients based on their likely response to DOX-based therapies. For instance, high CD133 expression in F5 subline cells correlates with higher DOX uptake, suggesting its potential as a predictive marker. In addition, variability in DOX uptake among TNBC sublines supports personalized medicine approaches. By evaluating a patient's tumor phenotypes, clinicians can design personalized treatment plans, optimizing drug selection and dosing to improve outcomes and reduce adverse effects. Overall, this study on DOX uptake in TNBC sublines offers critical insights for improving cancer treatment strategies. By targeting specific tumor subpopulations, addressing microenvironmental influences, and utilizing predictive biomarkers, we can advance towards more effective and personalized cancer therapies, overcoming drug resistance and enhancing chemotherapy success.

Conclusions

The intratumor diversity and microenvironmental factors explored in our study underline the complexity of treatment resistance in TNBC. By understanding how specific phenotypic properties contribute to drug uptake and resistance, we can tailor the development of targeted therapies and combination treatments. In this study, we revealed that phenotypically different cells exhibit varying DOX accumulation, with sensitive sublines showing higher nuclear accumulation and resistant sublines showing lower levels. Both 2D and 3D models confirmed that hypoxia reduces DOX accumulation. Modulating the TME, for instance, improving oxygenation or targeting hypoxic cells, could enhance the efficacy of conventional chemotherapies such as DOX. Our findings advocate for a personalized approach in TNBC treatment, where therapies are adapted based on the detailed characteristics of each tumour's subpopulation and its microenvironment. Ultimately, this study enriches our understanding of TNBC heterogeneity and emphasizes the importance of considering intratumor diversity and the TME in searching for more effective treatment strategies.

Acknowledgements

This research was supported by the Science Foundation of Lithuania University of Health Sciences project "Implication of interactions between triple-negative breast cancer cell populations for chemotherapy resistance", 2023.

Disclosure of conflict of interest

None.

Address correspondence to: Vilma Petrikaitė, Laboratory of Drug Targets Histopathology, Institute of Cardiology, Lithuanian University of Health Sciences, Sukileliu pr. 13, LT-50162 Kaunas, Lithuania. Tel: +370-686-29383; E-mail: vilma.petrikaite@lsmuni.lt

References

[1] Chen Y, Feng X, Yuan Y, Jiang J, Zhang P and Zhang B. Identification of a novel mechanism for reversal of doxorubicin-induced chemotherapy resistance by TXNIP in triple-negative breast cancer via promoting reactive oxygen-mediated DNA damage. Cell Death Dis 2022; 13: 338.

[2] Álvarez-Teijeiro S, García-Inclán C, Villaronga MÁ, Casado P, Hermida-Prado F, Granda-Díaz R, Rodrigo JP, Calvo F, del-Río-Ibisate N, Gandarillas A, Morís F, Hermsen M, Cutillas P and García-Pedrero JM. Factors secreted by cancer-associated fibroblasts that sustain cancer stem properties in head and neck squamous carcinoma cells as potential therapeutic targets. Cancers (Basel) 2018; 10: 334.

[3] Theile D and Wizgall P. Acquired ABC-transporter overexpression in cancer cells: transcriptional induction or Darwinian selection? Naunyn Schmiedebergs Arch Pharmacol 2021; 394: 1621-32.

[4] Hraběta J, Belhajová M, Šubrtová H, Merlos Rodrigo MA, Heger Z and Eckschlager T. Drug sequestration in lysosomes as one of the mechanisms of chemoresistance of cancer cells and the possibilities of its inhibition. Int J Mol Sci 2020; 21: 4392.
[5] Paškevičiūtė M and Petrikaitė V. Proton pump inhibitors modulate transport of doxorubicin and its liposomal form into 2D and 3D breast cancer cell cultures. Cancer Manag Res 2019; 11: 9761-69.
[6] Mattioli R, Ilari A, Colotti B, Mosca L, Fazi F and Colotti G. Doxorubicin and other anthracyclines in cancers: activity, chemoresistance and its overcoming. Mol Aspects Med 2023; 93: 101205.
[7] Chen Z, Han F, Du Y, Shi H and Zhou W. Hypoxic microenvironment in cancer: molecular mechanisms and therapeutic interventions. Signal Transduct Target Ther 2023; 8: 70.
[8] Ni Y, Zhou X, Yang J, Shi H, Li H, Zhao X and Ma X. The role of tumor-stroma interactions in drug resistance within tumor microenvironment. Front Cell Dev Biol 2021; 9: 637675.
[9] Deshmukh S and Saini S. Phenotypic heterogeneity in tumor progression, and its possible role in the onset of cancer. Front Genet 2020; 11: 604528.
[10] Bhattacharya S, Mohanty A, Achuthan S, Kotnala S, Jolly MK, Kulkarni P and Salgia R. Group behavior and emergence of cancer drug resistance. Trends Cancer 2021; 7: 323-34.
[11] Sasaki A, Nagatake T, Egami R, Gu G, Takigawa I, Ikeda W, Nakatani T, Kunisawa J and Fujita Y. Obesity suppresses cell-competition-mediated apical elimination of RasV12-transformed cells from epithelial tissues. Cell Rep 2018; 23: 974-82.
[12] Madan E, Peixoto ML, Dimitrion P, Eubank TD, Yekelchyk M, Talukdar S, Fisher PB, Mi QS, Moreno E and Gogna R. Cell competition boosts clonal evolution and hypoxic selection in cancer. Trends Cell Biol 2020; 30: 967-78.
[13] Pelham CJ, Nagane M and Madan E. Cell competition in tumor evolution and heterogeneity: merging past and present. Semin Cancer Biol 2020; 63: 11-18.
[14] Freischel AR, Damaghi M, Cunningham JJ, Ibrahim-Hashim A, Gillies RJ, Gatenby RA and Brown JS. Frequency-dependent interactions determine outcome of competition between two breast cancer cell lines. Sci Rep 2021; 11: 4908.
[15] Hapach LA, Carey SP, Schwager SC, Taufalele PV, Wang W, Mosier JA, Ortiz-Otero N, McArdle TJ, Goldblatt ZE, Lampi MC, Bordeleau F, Marshall JR, Richardson IM, Li J, King MR and Reinhart-King CA. Phenotypic heterogeneity and metastasis of breast cancer cells. Cancer Res 2021; 81: 3649-63.
[16] Hapach LA, Wang W, Schwager SC, Pokhriyal D, Fabiano ED and Reinhart-King CA. Phenotypically sorted highly and weakly migratory triple negative breast cancer cells exhibit migratory and metastatic commensalism. Breast Cancer Res 2023; 25: 102.
[17] Kvokačková B, Remšík J, Jolly MK and Souček K. Phenotypic heterogeneity of triple-negative breast cancer mediated by epithelial-mesenchymal plasticity. Cancers (Basel) 2021; 13: 2188.
[18] Moreira MP, Brayner FA, Alves LC, Cassali GD and Silva LM. Phenotypic, structural, and ultrastructural analysis of triple-negative breast cancer cell lines and breast cancer stem cell subpopulation. Eur Biophys J 2019; 48: 673-84.
[19] Jing X, Yang F, Shao C, Wei K, Xie M, Shen H and Shu Y. Role of hypoxia in cancer therapy by regulating the tumor microenvironment. Mol Cancer 2019; 18: 157.
[20] Sørensen BS and Horsman MR. Tumor hypoxia: impact on radiation therapy and molecular pathways. Front Oncol 2020; 10: 562.
[21] Januškevičienė I and Petrikaitė V. Interaction of phenotypic sublines isolated from triple-negative breast cancer cell line MDA-MB-231 modulates their sensitivity to paclitaxel and doxorubicin in 2D and 3D assays. Am J Cancer Res 2023; 13: 3368-83.
[22] Čeponytė U, Paškevičiūtė M and Petrikaitė V. Comparison of NSAIDs activity in COX-2 expressing and non-expressing 2D and 3D pancreatic cancer cell cultures. Cancer Manag Res 2018; 10: 1543-51.
[23] Bao L, Hazari S, Mehra S, Kaushal D, Moroz K and Dash S. Increased expression of P-glycoprotein and doxorubicin chemoresistance of metastatic breast cancer is regulated by miR-298. Am J Pathol 2012; 180: 2490-503.
[24] Khan GN, Kim EJ, Shin TS and Lee SH. Heterogeneous cell types in single-cell-derived clones of MCF7 and MDA-MB-231 cells. Anticancer Res 2017; 37: 2343-54.
[25] Al Tameemi W, Dale TP, Al-Jumaily RMK and Forsyth NR. Hypoxia-modified cancer cell metabolism. Front Cell Dev Biol 2019; 7: 4.
[26] Pronina VV, Kostryukova LV, Bulko TV and Shumyantseva VV. Interaction of doxorubicin embedded into phospholipid nanoparticles and targeted peptide-modified phospholipid nanoparticles with DNA. Molecules 2023; 28: 5317.
[27] Jawad B, Poudel L, Podgornik R and Ching WY. Molecular mechanism and binding free energy of doxorubicin intercalation in DNA. Phys Chem Chem Phys 2019; 21: 3877-93.

[28] Chen NT, Wu CY, Chung CY, Hwu Y, Cheng SH, Mou CY and Lo LW. Probing the dynamics of doxorubicin-DNA intercalation during the initial activation of apoptosis by fluorescence lifetime imaging microscopy (FLIM). PLoS One 2012; 7: e44947.
[29] Kopecka J, Godel M, Dei S, Giampietro R, Belisario DC, Akman M, Contino M, Teodori E and Riganti C. Insights into p-glycoprotein inhibitors: new inducers of immunogenic cell death. Cells 2020; 9: 1033.
[30] Mirzaei S, Gholami MH, Hashemi F, Zabolian A, Farahani MV, Hushmandi K, Zarrabi A, Goldman A, Ashrafizadeh M and Orive G. Advances in understanding the role of P-gp in doxorubicin resistance: molecular pathways, therapeutic strategies, and prospects. Drug Discov Today 2022; 27: 436-55.
[31] Chen R, Niu M, Hu X and He Y. Targeting mitochondrial dynamics proteins for the treatment of doxorubicin-induced cardiotoxicity. Front Mol Biosci 2023; 10: 1241225.
[32] Kopsida M, Clavero AL, Khaled J, Balgoma D, Luna-Marco C, Chowdhury A, Nyman SS, Rorsman F, Ebeling Barbier C, Bergsten P, Lennernäs H, Hedeland M and Heindryckx F. Inhibiting the endoplasmic reticulum stress response enhances the effect of doxorubicin by altering the lipid metabolism of liver cancer cells. Mol Metab 2024; 79: 101846.
[33] Lin CP, Wu SH, Lin TY, Chu CH, Lo LW, Kuo CC, Chang JY, Hsu SC, Ko BS, Yao M, Hsiao JK, Wang SW and Huang DM. Lysosomal-targeted doxorubicin delivery using RBC-derived vesicles to overcome drug-resistant cancer through mitochondrial-dependent cell death. Pharmacol Res 2023; 197: 106945.
[34] dos Reis SB, de Oliveira Silva J, Garcia-Fossa F, Leite EA, Malachias A, Pound-Lana G, Mosqueira VCF, Oliveira MC, de Barros ALB and de Jesus MB. Mechanistic insights into the intracellular release of doxorubicin from pH-sensitive liposomes. Biomed Pharmacother 2021; 134: 110952.
[35] Cohen O and Granek R. Nucleus-targeted drug delivery: theoretical optimization of nanoparticles decoration for enhanced intracellular active transport. Nano Lett 2014; 14: 2515-21.
[36] Brancato V, Gioiella F, Imparato G, Guarnieri D, Urciuolo F and Netti PA. 3D breast cancer microtissue reveals the role of tumor microenvironment on the transport and efficacy of free-doxorubicin in vitro. Acta Biomater 2018; 75: 200-12.
[37] Sztankovics D, Moldvai D, Petővári G, Gelencsér R, Krencz I, Raffay R, Dankó T and Sebestyén A. 3D bioprinting and the revolution in experimental cancer model systems-A review of developing new models and experiences with in vitro 3D bioprinted breast cancer tissue-mimetic structures. Pathol Oncol Res 2023; 29: 1610996.
[38] Prasetyanti PR and Medema JP. Intra-tumor heterogeneity from a cancer stem cell perspective. Mol Cancer 2017; 16: 41.
[39] Yang F, Cao L, Sun Z, Jin J, Fang H, Zhang W and Guan X. Evaluation of breast cancer stem cells and intratumor stemness heterogeneity in triple-negative breast cancer as prognostic factors. Int J Biol Sci 2016; 12: 1568-77.
[40] Saha T and Lukong KE. Breast cancer stem-like cells in drug resistance: a review of mechanisms and novel therapeutic strategies to overcome drug resistance. Front Oncol 2022; 12: 856974.
[41] Yu S, Zheng J, Zhang Y, Meng D, Wang Y, Xu X, Liang N, Shabiti S, Zhang X, Wang Z, Yang Z, Mi P, Zheng X, Li W and Chen H. The mechanisms of multidrug resistance of breast cancer and research progress on related reversal agents. Bioorg Med Chem 2023; 95: 117486.
[42] Tang K, Zhu L, Chen J, Wang D, Zeng L, Chen C, Tang L, Zhou L, Wei K, Zhou Y, Lv J, Liu Y, Zhang H, Ma J and Huang B. Hypoxia promotes breast cancer cell growth by activating a glycogen metabolic program. Cancer Res 2021; 81: 4949-63.
[43] Gilkes DM, Semenza GL and Wirtz D. Hypoxia and the extracellular matrix: drivers of tumour metastasis. Nat Rev Cancer 2014; 14: 430-9.
[44] Weigelt B, Ghajar CM and Bissell MJ. The need for complex 3D culture models to unravel novel pathways and identify accurate biomarkers in breast cancer. Adv Drug Deliv Rev 2014; 69-70: 42-51.
[45] Aydinlik S, Erkisa M, Cevatemre B, Sarimahmut M, Dere E, Ari F and Ulukaya E. Enhanced cytotoxic activity of doxorubicin through the inhibition of autophagy in triple negative breast cancer cell line. Biochim Biophys Acta Gen Subj 2017; 1861: 49-57.
[46] Engle K and Kumar G. Cancer multidrug-resistance reversal by ABCB1 inhibition: a recent update. Eur J Med Chem 2022; 239: 114542.
[47] Kinnel B, Singh SK, Oprea-Ilies G and Singh R. Targeted therapy and mechanisms of drug resistance in breast cancer. Cancers (Basel) 2023; 15: 1320.
[48] Jianmongkol S. Overcoming P-glycoprotein-mediated doxorubicin resistance. In: Arnouk H, editors. Advances in Precision Medicine Oncology. IntechOpen; 2021. pp. 1-22.
[49] Fultang N, Chakraborty M and Peethambaran B. Regulation of cancer stem cells in triple negative breast cancer. Cancer Drug Resist 2021; 4: 321-42.
[50] Cheng CC, Shi LH, Wang XJ, Wang SX, Wan XQ, Liu SR, Wang YF, Lu Z, Wang LH and Ding Y.

Stat3/Oct-4/c-Myc signal circuit for regulating stemness-mediated doxorubicin resistance of triple-negative breast cancer cells and inhibitory effects of WP1066. Int J Oncol 2018; 53: 339-48.

[51] Tsou SH, Chen TM, Hsiao HT and Chen YH. A critical dose of doxorubicin is required to alter the gene expression profiles in MCF-7 cells acquiring multidrug resistance. PLoS One 2015; 10: e0116747.

[52] Otter M, Csader S, Keiser M and Oswald S. Expression and functional contribution of different organic cation transporters to the cellular uptake of doxorubicin into human breast cancer and cardiac tissue. Int J Mol Sci 2021; 23: 255.

[53] Kullenberg F, Degerstedt O, Calitz C, Pavlović N, Balgoma D, Gråsjö J, Sjögren E, Hedeland M, Heindryckx F and Lennernäs H. In vitro cell toxicity and intracellular uptake of doxorubicin exposed as a solution or liposomes: implications for treatment of hepatocellular carcinoma. Cells 2021; 10: 1717.

[54] Nagai K, Fukuno S, Shiota M, Tamura M, Yabumoto S and Konishi H. Differences in transport characteristics and cytotoxicity of epirubicin and doxorubicin in HepG2 and A549 cells. Anticancer Res 2021; 41: 6105-12.

[55] Lei T, Srinivasan S, Tang Y, Manchanda R, Nagesetti A, Fernandez-Fernandez A and McGoron AJ. Comparing cellular uptake and cytotoxicity of targeted drug carriers in cancer cell lines with different drug resistance mechanisms. Nanomedicine 2011; 7: 324-32.